arXiv:nucl-th/0306083v1 29 Jun 2003

Oblate-prolate transition in odd-mass light mercury isotopes

Shouichi Sakakihara* and Yasutoshi Tanaka

Department of Environmental Technology and Urban Planning,

Nagoya Institute of Technology, Gokiso, Nagoya 466-8555, Japan

February 5, 2008

Abstract

Anomalous isotope shifts in the chain of light Hg isotopes are investigated by using the Hartree-Fock-Bogoliubov method with the Skyrme SIII, SkI3 and SLy4 forces. The sharp increase in the mean-square radius of the odd mass $^{181-185}$Hg isotopes is well explained in terms of the transition from an oblate to a prolate shape in the ground state of these isotopes. We discuss the polarization energy of time-odd mean-field terms in relation to the blocked level by the odd neutron.

PACS: 21.10.Dr; 21.10.Ft; 21.10.Ma; 21.60.Jz

Keywords: isotope shifts; shape coexistence; Hartree-Fock-Bogoliubov method; Lipkin-Nogami corrections; time-odd mean fields

1 Introduction

The sharp increase in the mean-square charge radius is observed in the odd mass $^{181-185}$Hg isotopes with respect to their even neighbors [1]. A hint that a very different configuration may constitute the ground state of these nuclei was given by an isomer shift measurement of ^{185}Hg [2], where they found an excited state of ^{185}Hg which has a charge radius consistent with the charge radius of heavier neighbors. The sharp increase in the charge radius was interpreted as the transition from a nearly spherical to a deformed shape in the ground state of the odd mass $^{181-185}$Hg isotopes.

* *e-mail address* : shouichi@npl.kyy.nitech.ac.jp

Frauendorf and Pashkevich [3] calculated the deformation energy of Hg isotopes by means of Strutinsky's shell correction method. They found that the light Hg isotope has an oblate and prolate minimum of nearly the same depth at the respective deformations $\epsilon = -0.12$ and 0.22. They discussed a mechanism which causes the transition from a small oblate to a large prolate deformation in the odd mass $^{181-185}$Hg isotopes. They noticed that the neutron level density is very high in the almost spherical oblate minimum, whereas the neutron level density is low in the well deformed prolate minimum. They concluded that the loss of pairing energy due to the blocking of the Fermi level by the odd neutron is larger in the oblate minimum than in the prolate one, which gives rise to the oblate-prolate transition in the ground state of these isotopes. As the prolate minimum corresponds to deformation twice as large as the oblate one, the sharp increase in the mean-square radius is observed in the odd-mass light Hg isotopes.

There are several mean field calculations of Hg isotopes. However, all of them are limited to even isotopes [4, 5, 6, 7]. In order to see if the mechanism of Frauendorf and Pashkevich works well, we perform Hartree-Fock-Bogoliubov (HFB) calculations of Hg isotopes with effective interactions SIII [8], SkI3 [9] and SLy4 [10]. We calculate Lipkin-Nogami corrections [11, 12] to both mean field and pairing energies [13, 14]. We investigate the influence of the time-odd mean-field terms as well as the blocking of a level by the odd neutron on the oblate-prolate shape transition.

In Section 2, we present the Skyrme HFB method with Lipkin-Nogami corrections to describe both even and odd Hg isotopes. In Section 3, we present calculations with effective interactions SIII, SkI3 and SLy4. Conclusions are given in Section 4.

2 Method of calculation

2.1 Skyrme Hartree-Fock-Bogoliubov method

The HFB equation is derived by the variation of energy with respect to the quasi-particle vacuum [15],

$$H = \sum_{\alpha\beta} t_{\alpha\beta} {c_\alpha}^\dagger c_\beta + \frac{1}{4} \sum_{\alpha\beta\gamma\delta} \bar{v}_{\alpha\beta\gamma\delta} {c_\alpha}^\dagger {c_\beta}^\dagger c_\delta c_\gamma, \tag{1}$$

$$\delta \frac{\langle\Phi|H|\Phi\rangle}{\langle\Phi|\Phi\rangle} = 0. \tag{2}$$

Here the quasi-particle vacuum $|\Phi\rangle$ is given by

$$\beta_k = \sum_\alpha U^*_{\alpha k} c_\alpha + V^*_{\alpha k} {c_\alpha}^\dagger, \tag{3}$$

$$\beta_k |\Phi\rangle = 0 \tag{4}$$

for all quasi-particle states k. In the present study, we employ Skyrme forces in the particle-hole channel and the zero-range density-dependent pairing force in the particle-particle channel,

$$V_p = \frac{V_0}{2}\left(1 - P_\sigma\right)\left(1 - \frac{\rho(\boldsymbol{r_1})}{\rho_{\rm c}}\right)\delta(\boldsymbol{r_1} - \boldsymbol{r_2}). \tag{5}$$

The HFB energy is then given by

$$E^{\rm HFB} = \int \mathcal{H} d\boldsymbol{r} + \frac{1}{2}\int \Delta(\boldsymbol{r})\kappa^*(\boldsymbol{r}) d\boldsymbol{r}, \tag{6}$$

where $\mathcal{H}$ is the Skyrme energy density [16, 17] and $\Delta(\boldsymbol{r})$ is the gap field,

$$\Delta(\boldsymbol{r}) = \frac{V_0}{2}\left(1 - \frac{\rho(\boldsymbol{r})}{\rho_{\rm c}}\right)\kappa(\boldsymbol{r}). \tag{7}$$

The pairing strength V_0 is determined from the odd-even mass difference and the density parameter $\rho_{\rm c}$ is taken as the saturation density of symmetric nuclear matter which is obtained by using the respective Skyrme parameters. The particle density $\rho(\boldsymbol{r})$ and the anomalous density $\kappa(\boldsymbol{r})$ are written as

$$\rho(\boldsymbol{r}\sigma, \boldsymbol{r}\sigma') = \sum_{\alpha\beta} \rho_{\alpha\beta}\varphi_\alpha(\boldsymbol{r}, \sigma)\varphi^*_\beta(\boldsymbol{r}, \sigma'), \tag{8}$$

$$\kappa(\boldsymbol{r}\sigma, \boldsymbol{r}\sigma') = \sum_{\alpha\beta} \kappa_{\alpha\beta}\varphi_\alpha(\boldsymbol{r}, \sigma)\varphi_\beta(\boldsymbol{r}, \sigma') \tag{9}$$

with the density matrix and pairing tensor,

$$\rho_{\alpha\beta} = \langle\Phi|{c_\beta}^\dagger c_\alpha|\Phi\rangle = \sum_k V^*_{\alpha k} V_{\beta k}, \tag{10}$$

$$\kappa_{\alpha\beta} = \langle\Phi|c_\beta c_\alpha|\Phi\rangle = \sum_k V^*_{\alpha k} U_{\beta k}. \tag{11}$$

Variation of Eq. (6) with respect to $\rho_{\alpha\beta}$ and $\kappa_{\alpha\beta}$ yields the HFB equation,

$$\begin{pmatrix} h_{\alpha\beta} - \lambda\delta_{\alpha\beta} & \Delta_{\alpha\beta} \\ -\Delta^*_{\alpha\beta} & -h^*_{\alpha\beta} + \lambda\delta_{\alpha\beta} \end{pmatrix} \begin{pmatrix} U_{\beta k} \\ V_{\beta k} \end{pmatrix} = E_k \begin{pmatrix} U_{\alpha k} \\ V_{\alpha k} \end{pmatrix}. \tag{12}$$

Diagonalization is carried out in a deformed oscillator basis with axial symmetry [18]. A Greek index in Eq. (12) denotes a set of quantum numbers $\{n_r n_z \Lambda\Sigma\}$ of a deformed oscillator wave function.

In the present study we will restrict our basis space as

$$E_\alpha = (2n_r + |\Lambda| + 1)\hbar\omega_\perp + \left(n_z + \frac{1}{2}\right)\hbar\omega_z \leq \left(N_0 + \frac{3}{2}\right)\hbar\omega_0 \tag{13}$$

with $N_0 = 18$. The oscillator constant is held fixed as $\hbar\omega_0 = \hbar(\omega_\perp^2\omega_z)^{1/3} = 1.21 \times \frac{\hbar^2}{m}A^{-1/3}$. The deformation parameter $q = \omega_\perp/\omega_z$ is varied to obtain the maximum deformation energy in the oblate and prolate minimum, respectively. The chemical potential λ is adjusted by the particle number condition, $\langle\hat{N}\rangle = N$. Using the occupation amplitude $N_k = \sum_\alpha V_{\alpha k}^* V_{\alpha k}$ and quasi-particle energy E_k, we calculate an auxiliary single-particle energy and pairing gap in order to find the optimum value of λ [19],

$$\bar{e}_k = -E_k(2N_k - 1) + \lambda, \tag{14}$$

$$\bar{\Delta}_k = 2E_k\sqrt{N_k(1 - N_k)}. \tag{15}$$

As in Ref. [20, 21], the cut-off procedure of quasi-particle states is imposed on the auxiliary single-particle energy. The value of $\bar{e}_{\max} = 60$ MeV is assumed in the present study.

2.2 Description of an odd nucleus

The above formalism can be straightforwardly extended to the case of one quasi-particle state in odd mass nuclei. All the equation retain their form. Only the density matrix $\rho_{\alpha\beta}$ and pairing tensor $\kappa_{\alpha\beta}$ should be modified due to the blocked quasi-particle $\beta_k^\dagger|\Phi\rangle$ in the following way [22, 23];

$$\tilde{\rho}_{\alpha\beta} = \rho_{\alpha\beta} + U_{\alpha k}U_{\beta k}^* - V_{\alpha k}^* V_{\beta k}, \tag{16}$$

$$\tilde{\kappa}_{\alpha\beta} = \kappa_{\alpha\beta} + U_{\alpha k}V_{\beta k}^* - V_{\alpha k}^* U_{\beta k}. \tag{17}$$

We introduce a reference state $|\Phi_{\rm HFBE}\rangle$ and its energy expectation value $E^{\rm HFBE}$. The state is constructed as an *even* vacuum without quasi-particle creation and without breaking time-reversal invariance but with an *odd* average particle number. The difference of energy $E^{\rm HFB} - E^{\rm HFBE}$ is thus composed of the loss of pairing energy due to the blocking of the Fermi level and the polarization energy of the mean field by the presence of an odd neutron [24].

A proper description of an odd nucleus by mean field theories requires to break the time-reversal symmetry [17]. When the time-reversal symmetry is broken, the Skyrme energy density $\mathcal{H}$ is written by the sum of kinetic

energy and potential energy of isoscalar $\mathcal{H}_0$ and isovector $\mathcal{H}_1$ terms;

$$\begin{aligned}
\mathcal{H} &= \frac{\hbar^2}{2m}\tau_0 + \mathcal{H}_0 + \mathcal{H}_1, \\
\mathcal{H}_t &= C_t^{\rho}\rho_t^2 + C_t^{s}\boldsymbol{s}_t^2 + C_t^{\triangle\rho}\rho_t\triangle\rho_t + C_t^{\triangle s}\boldsymbol{s}_t\cdot\triangle\boldsymbol{s}_t \\
&\quad + C_t^{\tau}(\rho_t\tau_t - \boldsymbol{j}_t^2) + C_t^{J}(\boldsymbol{J}_t^2 - \boldsymbol{s}_t\cdot\boldsymbol{T}_t) + C_t^{\nabla J}[\rho_t\nabla\cdot\boldsymbol{J}_t + \boldsymbol{s}_t\cdot(\nabla\times\boldsymbol{j}_t)].
\end{aligned} \tag{18}$$

The coupling constants C are expressed by the Skyrme force parameters [25]. The isospin index t can have values 0 or 1. The isoscalar and isovector parts of the particle densities ρ_t are defined as

$$\rho_0 = \rho_n + \rho_p, \qquad \rho_1 = \rho_n - \rho_p, \tag{19}$$

and analogous expressions are used to define other densities. It should be noted that since we consider the Skyrme force as the density-dependent two-body interaction, the time-odd terms C_t^s in Eq. (18) are different from the original expressions [17] which were derived from the three-body interaction.

The characteristic combinations of $(\rho_t\tau_t - \boldsymbol{j}_t^2)$, $(\boldsymbol{J}_t^2 - \boldsymbol{s}_t\cdot\boldsymbol{T}_t)$ and $[\rho_t\nabla\cdot\boldsymbol{J}_t + \boldsymbol{s}_t\cdot(\nabla\times\boldsymbol{j}_t)]$ in Eq. (18) are the results of the local gauge invariance of the Skyrme force [25]. The time-odd coupling constants are uniquely determined from the original Skyrme-force parameters and therefore the time-odd mean field has no adjustable parameters once the time-even mean field is given. However, as discussed by Dobaczewski and Dudek [25], one may consider the energy density to be a more fundamental construction than the Skyrme interaction itself. In such a case, all 20 coupling constants in Eq. (18) can be treated and adjusted independently. However, the gauge-invariant conditions restrict the values of six time-odd coupling constants and leave the freedom to modify the values of C_t^s and $C_t^{\Delta s}$. We are going to vary C_t^s and $C_t^{\Delta s}$ to see the influence of these terms on the oblate-prolate transition in the odd-mass $^{181-185}$Hg isotopes. We will omit the terms $(\boldsymbol{J}_t^2 - \boldsymbol{s}_t\cdot\boldsymbol{T}_t)$ because $\boldsymbol{J}_t^2$ are omitted in the parameterization of the present Skyrme forces.

2.3 Lipkin-Nogami corrections

In light Hg isotopes, the neutron level density is high in the oblate minimum, while it is low in the prolate minimum. Because of the difference of level densities in the respective minima, it happens that neutrons in the oblate minimum are superconductive, whereas they are normal in the prolate minimum within the same isotope. The situation is extremely inconvenient because we want discuss the energy difference between the oblate and prolate minimum. Besides, a sudden phase-transition from the normal to superconductive state or vice versa

at certain neutron numbers may be unphysical and it may be due to the defect of the number non-conserving pairing scheme. In the present study we employ the approximate number-projection method of Lipkin and Nogami (LN) [11, 12] and calculate its corrections to both mean field and pairing energies [13]. The number projected energy is expressed as

$$E_{\rm HFBLN} = E_{\rm HFB} + \lambda_1(N - \langle\hat{N}\rangle) + \lambda_2(N^2 - \langle\hat{N}^2\rangle) + \cdots, \tag{20}$$

where λ_1 and λ_2 are constant parameters [14]. The second order expansion is considered in the Lipkin-Nogami method. Variation with respect to the density matrix and pairing tensor as in the case of the HFB equation yields the HFBLN equation applicable to both even and odd nuclei (hereafter simply called HFB). The parameter λ_1 is given by the particle number condition, whereas the parameter λ_2 is held fixed during the variation and is determined after the variation from the additional condition,

$$|\xi\rangle = \exp(i\xi\hat{N}_{20})|\Phi\rangle, \tag{21}$$

$$\lambda_2 = \frac{\partial_\xi^2\langle\Phi|H|\xi\rangle\Big|_{\xi=0}}{\partial_\xi^2\langle\Phi|\hat{N}^2|\xi\rangle\Big|_{\xi=0}}. \tag{22}$$

Equation (22) is calculated by the following density matrix and pairing tensor [13];

$$\rho^{(\xi)}_{\alpha\beta} = \langle\Phi|c^\dagger_\beta c_\alpha|\xi\rangle = (\rho + 2i\xi(1-\rho)\rho)_{\alpha\beta}\,, \tag{23}$$

$$\kappa^{(\xi)}_{\alpha\beta} = \langle\Phi|c_\beta c_\alpha|\xi\rangle = (\kappa + 2i\xi(1-\rho)\kappa)_{\alpha\beta}\,, \tag{24}$$

$$\bar{\kappa}^{(\xi)}_{\alpha\beta} = \langle\Phi|c^\dagger_\alpha c^\dagger_\beta|\xi\rangle = (\kappa^* - 2i\xi\kappa^*\rho)_{\alpha\beta}. \tag{25}$$

For an odd nucleus, the density matrix and pairing tensor of Eqs. (16) and (17) are used on the right hand side of the above equations [14].

3 Results and discussion

We have analysed the oblate-prolate transition in the odd-mass light Hg isotopes using the Skyrme Hartree-Fock-Bogoliubov method with effective interactions SIII, SkI3 and SLy4. Shape transition occurs only in the odd-mass isotopes as the result of a subtle balance between the time-even mean-field energy, the loss of pairing energy by the odd neutron and the time-odd mean-field energy. We have examined effective interactions SIII, SGII [26], SkM* [27], SKX [28], SkI1, SkI2, SkI3, SkI4 and SkI5 [9] and SLy4 whether they can predict the

oblate-prolate shape coexistence in light Hg isotopes. We have found that both SIII and SkI3 interactions have desirable isospin dependence and deformation energies.

We have assumed the zero-range density-dependent pairing interaction. The pairing strength V_0 was adjusted to reproduce the one-particle separation energy [29]. The density parameter ρ_c is taken as the saturation density of symmetric nuclear matter which is obtained from Skyrme parameters. Adjusted values are given in the respective figure captions.

We have investigated the effect of time-odd mean-field terms on the HFB energy, first by using the time-odd coupling constants derived from the Skyrme force parameters and second by switching on and off the coupling constants $C_t^{\Delta s}$ and C_t^s, respectively. These coupling constants in C-representation [25] are given in Table 1. They vary very much with different Skyrme forces, e.g., the coupling constant $C_0^s(\rho = 0)$ is 14, 84 and –208 for the respective SIII, SkI3 and SLy4 forces.

The polarization energy depends strongly on the blocked level by an odd neutron. Even the sign of energy changes with different choice of the blocked level. In the present study we simply choose as the blocked level the lowest quasi-particle state that is obtained from the HFBE calculation.

Mercury isotopes are very interesting because the shape of the ground state varies very much as the neutron number decreases from the closed shell. Figure 1 shows the deformation energy of even Hg isotopes calculated by the constraint SIII-HF method. We see the spherical shape in the neutron-closed ^{206}Hg. The oblate minimum with deformation $\beta_2 \sim -0.17$ then develops in ^{200}Hg. A rather complicated prolate minimum appears in ^{190}Hg. Finally the deep prolate minimum with deformation $\beta_2 \sim 0.29$ develops in ^{184}Hg. The oblate-prolate shape coexistence in light Hg isotopes has been predicted by many authors, e.g., [3, 4, 5, 6, 7, 30, 31].

Figure 2 shows the SIII calculation of the oblate-prolate energy difference. The HF calculation (white circle) predicts prolate deformation in the ground state of all Hg isotopes. The HFBE calculation (black circle), the fully paired state without the blocking effect, predicts oblate deformation in the ground state of all Hg isotopes. The shape changes due to the large gain of pairing energy in the oblate minimum because of the high level density as compared to the level density in the prolate minimum. In the SIII-HFB calculation (white square), on the other hand, the shape of odd mass $^{181-185}$Hg isotopes returns to the prolate shape. This is because the loss of pairing energy due to the blocking by the odd neutron is also large in the oblate minimum than in the prolate one. The effect of the time-odd mean fields on the oblate-prolate transition is weak and a few tenths of the blocking effect.

Figure 3 shows the SIII-HFB calculation of (a) the mean-square charge radius and (b) one-neutron separation energy of $^{180-206}$Hg isotopes. The sharp increase in the mean-square radius of the odd-mass $^{181-185}$Hg isotopes is very well explained by the calculation. The one-neutron separation energy is also well reproduced in the calculation. This is so because the depth of the pairing force has been adjusted to reproduce the observed separation energies. It is noted that the white circle in Fig. 3(b) is a derived value from systematic trends [29] and not an experiment.

As is well known, a proper description of odd nuclei by mean field theory requires to break the time-reversal symmetry and introduces the time-odd components (TOC) in the mean field. The effect of an odd neutron on the HFB energy is therefore twofold; (a) The loss of pairing energy due to the blocking of the Fermi level by the odd neutron, and (b) the time-odd mean-field energy arising from the blocked level. The time-odd mean fields have been studied both in the analysis of super-deformed rotational bands [25] and the odd-even nuclear mass difference [24].

In order to see the blocking energy (the loss of pairing energy) and the polarization energy (the time-odd mean-field energy) separately, we define the blocking energy $E^{\rm block}$ as the energy difference between $E^{\rm HFB}$ with no TOC and $E^{\rm HFBE}$. We also define the polarization energy $E^{\rm pol}$ as the energy difference between $E^{\rm HFB}$ and $E^{\rm HFB}$ with no TOC, i.e.,

$$E^{\rm block} = E^{\rm HFB}(\text{no TOC}) - E^{\rm HFBE}, \tag{26}$$

$$E^{\rm pol} = E^{\rm HFB} - E^{\rm HFB}(\text{no TOC}). \tag{27}$$

Figure 4 shows the SIII-HFB calculation of (a) the blocking energy in the oblate and prolate minimum, (b) the polarization energy in the oblate minimum, (c) the polarization energy in the prolate minimum and (d) the oblate-prolate difference of HFB energy. In Fig. 4(a), the blocking energy in the oblate minimum is larger by $\sim$200 keV than the one in the prolate minimum. This results from higher neutron level-density in the former than in the latter. The blocking energies are reversed in ^{189}Hg because of the small deformation $\beta = 0.08$ in the prolate minimum of this isotope and the level density in the minimum is high accordingly.

As mentioned in Section 2.2, the C_t^s and $C_t^{\triangle s}$ terms are free from the time-even parameterization. To investigate their effects on the HFB energy, we have further divided the polarization energy into contributions with (i) the full time-odd terms, (ii) the time-odd terms without C_t^s, (iii) the time-odd terms without $C_t^{\Delta s}$, and (iv) the time-odd terms without both C_t^s and $C_t^{\Delta s}$. In the following we assume simultaneous modifications of

the isoscalar and isovector coupling constants of a given species.

Figures 4 (b) and (c) display the contributions to the polarization energy. The polarization energy with full time-odd terms (white circle) is quite small. It is attractive and less than –50 keV in the oblate minimum, while it is repulsive and less than 50 keV in the prolate minimum. When the C_t^s terms are omitted (black circle), the polarization energy becomes attractive and more than –250 keV in the oblate minimum and it is attractive around –150 keV in the prolate minimum. The C_t^s terms have repulsive contribution to the HFB energy. When the $C_t^{\Delta s}$ terms are omitted (white square), on the other hand, the polarization energy becomes repulsive and ∼50 keV in both minima. The $C_t^{\Delta s}$ terms have large attractive contributions to the HFB energy. When both C_t^s and $C_t^{\Delta s}$ terms are omitted (black square), the polarization energy becomes small. The effect of the C_t^s and $C_t^{\Delta s}$ terms is opposite and cancels with each other.

Figure 4(d) shows the difference of energy in the oblate and prolate minimum. The figure shows the calculation with the full time-odd terms (white circle), without the C_t^s terms (black circle), without the $C_t^{\Delta s}$ terms (white square), without both C_t^s and $C_t^{\Delta s}$ terms (black square) and without all time-odd terms (white triangle). When both C_t^s and $C_t^{\Delta s}$ terms are omitted, the oblate shape is predicted in ^{181}Hg, while the prolate shape is calculated in ^{185}Hg with marginal energy difference between the oblate and prolate minima.

Table 2 summarizes the oblate-prolate difference of the HFBE energy $\Delta E^{\rm HFBE}$, the blocking energy $\Delta E^{\rm block}$, the polarization energy $\Delta E^{\rm pol}$ and the sum of these contributions $\Delta E^{\rm HFB}$. The polarization energy $\Delta E^{\rm pol}$ is calculated with four different time-odd mean fields. They are the HFB calculation (i) with full time-odd terms, (ii) without the C_t^s terms, (iii) without the $C_t^{\Delta s}$ terms and (iv) without both C_t^s and $C_t^{\Delta s}$ terms.

The energy difference $\Delta E^{\rm HFBE}$ shows that the minimum is found at the neutron number $N = 102$ and the oblate minimum gets deeper than the prolate one as the neutron number is away from $N = 102$ in both directions. For the blocking energy $E^{\rm block}$, it is repulsive and larger by 400 keV in the oblate minimum than in the prolate one. The blocked level is labeled with the quantum number Ω, the component of neutron angular momentum along the symmetry axis.

For the odd mass $^{181-185}$Hg, the blocked level has $\Omega = 1/2$ in the oblate minimum, while it has $\Omega = 5/2$ or $7/2$ in the prolate minimum. In the calculation with full time-odd terms (case (i)), the polarization energy is attractive in the oblate minimum, while it is repulsive in the prolate minimum, leading to the the attractive energy difference of $\Delta E^{\rm pol}$. The attractive $\Delta E^{\rm pol}$ weakens the repulsive $\Delta E^{\rm block}$ and prevents the oblate-prolate shape transition in these isotopes. In the calculation without the C_t^s terms (case (ii)), the polarization energy

becomes attractive because of the absence of the repulsive C_t^s terms. In this case, the polarization energy $\Delta E^{\rm pol}$ almost cancels the blocking energy $\Delta E^{\rm block}$. In the calculation without the $C_t^{\Delta s}$ terms (case (iii)), the polarization energy is weakly repulsive because of the absence of strongly attractive $C_t^{\Delta s}$ terms. Finally in the calculation without both C_t^s and $C_t^{\Delta s}$ terms, the polarization energy is weakly attractive in both minima. The effects of the C_t^s and $C_t^{\Delta s}$ terms on the polarization energy will be discussed more generally in the last paragraph of this section.

Figure 5 shows the results of the SkI3-HFB calculation. We had the difficulty of convergence in this calculation when the full time-odd components are considered. The difficulty arises mainly due to the strong coupling-constant $C_0^{\Delta s}$ derived from the SkI3 parameters (see Table 1) and partly due to the large HF basis of the present study ($N_0 = 18$). The difficulty occurs when the energy splitting between the time-reversed partners becomes large and a few of the quasi-particle states have negative energy. Since we have no way to correct this difficulty, we simply omit the $C_t^{\Delta s}$ terms and display the results in Fig. 5. The blocking energy $E^{\rm block}$ in Fig. 5(a) is similar to the one in the SIII-HFB calculation. Figures 5(b) and 5(c) show the polarization energy (iii) without $C_t^{\Delta s}$ terms (white square) and (iv) without both $C_t^{\Delta s}$ and C_t^s terms (black square). The C_t^s terms have repulsive contributions of $\sim$150 keV in the oblate minimum while it is $\sim$200 keV in the prolate minimum. In Fig. 5(d), the oblate-prolate transition is very well explained when the terms $C_t^{\Delta s}$ are omitted. It is also well explained by omitting the whole time-odd components.

Table 3 summarizes the results of the SkI3-HFB calculation. The energy difference $\Delta E^{\rm HFBE}$ is nearly the same for even and odd $^{180-185}$Hg isotopes. This fact helps very much in reproducing the oblate-prolate transition in the odd mass $^{181-185}$Hg isotopes. The SkI3 force is very well suited to describe the mean fields of light Hg isotopes.

Figure 6 shows the results of the SLy4-HFB calculation. The blocking energy $E^{\rm block}$ in the odd-mass $^{181-185}$Hg is larger by $\sim$200 keV in the oblate minimum than in the prolate one. However, their magnitudes are reversed at the neutron number $N = 107$ and $N = 109$. The reason is the same as the SIII calculation. The equilibrium deformation in the prolate minimum is reduced to $\beta = 0.12$ in these isotopes. Figures 6(b) and 6(c) show the terms C_t^s have repulsive contributions to the polarization energy. In addition, the terms C_t^s and $C_t^{\Delta s}$ have opposite signs and nearly cancel with each other.

The oblate-prolate energy difference in Fig. 6(d) shows that the SLy4 force is not very well suited to describe deformation properties of light Hg isotopes. Here we also had the difficulty of convergence when the C_t^s terms are

not included in the calculation. The difficulty may be due to the $C_t^{\Delta s}$ terms. The repulsive C_t^s terms cancel the attractive $C_t^{\Delta s}$ terms. Without the C_t^s terms, the attractive $C_t^{\Delta s}$ terms are quite strong and cause the difficulty of convergence.

Table 4 summarizes the results of the SLy4-HFB calculation. The energy difference $\Delta E^{\rm HFBE}$ shows that the SLy4 force favors the oblate shape in light Hg isotopes much more than the SIII and SkI3 forces. This fact results in the oblate-prolate transition only in the ground state of ^{181}Hg isotope. The oblate shape is predicted for all heavier isotopes.

To see the effects of the time-odd C_t^s and $C_t^{\Delta s}$ terms more closely, we have analysed the odd-mass Sn, Ba, Yb, Hg and Pb isotopes by the SkI3-HFB method with the basis space of $N_0 = 10$. A small basis space was chosen in order to avoid the difficulty of convergence. Results of the SkI3-HF calculation are shown in Fig. 7. The polarization energy is plotted against $2 \times \Omega^\pi$ of the blocked level. Polarization energies are calculated (a) with the full time-odd terms, (b) without $C_t^{\Delta s}$ terms and (c) without both $C_t^{\Delta s}$ and C_t^s terms. We may conclude that the $C_t^{\Delta s}$ terms are attractive and have a large effect on the blocked level with low Ω, in particular $\Omega^\pi = 1/2^\pm$. The terms C_t^s are repulsive for levels with any value of Ω. The remaining time-odd terms are attractive for levels with high Ω and are negligible for levels with low Ω. The same features of the time-odd terms are observed also for the SIII and SLy4 interactions. For the odd-mass $^{181-185}$Hg in Tables 2, 3 and 4, we have seen that the time-odd terms have attractive contributions to $\Delta E^{\rm HFB}$ in the cases (i) and (ii), while the terms have repulsive contributions in the case (iv).

4 Conclusions

The shape and the mean-square radius of Hg isotopes have been investigated by using the Skyrme Hartree-Fock-Bogoliubov method. We have first examined effective interactions SIII, SGII, SkM*, SKX, SkI1, SkI2, SkI3, SkI4, SkI5 and SLy4 to see if they can predict the oblate-prolate shape coexistence in light Hg isotopes. We have then examined the loss of pairing energy due to the odd neutron by employing the zero-range density-dependent pairing force. Lipkin-Nogami corrections to both even and odd nuclei are calculated within the HFB formalism. We have also investigated the effect of the time-odd $C_t^{\Delta s}$ and C_t^s terms on the HFB energy in relation to the blocked level by the odd neutron.

We have obtained the following conclusions. (1) The effective interactions SIII and SkI3 have desirable

deformation properties in predicting the oblate-prolate shape coexistence in light Hg isotopes. (2) The blocking energy of the pairing is the most important factor to change the shape of the odd-mass $^{181-185}$Hg isotopes. (3) The effect of the time-odd terms on the prolate-oblate transition is weak and cancels the effect of the blocking energy by a few tenths.

We have also investigated the effects of the time-odd terms C_t^s and $C_t^{\Delta s}$ by blocking several levels near the Fermi surface of Sn, Ba, Yb, Hg and Pb isotopes. We have found that the terms $C_t^{\Delta s}$ are attractive for the blocked levels with low Ω, in particular $\Omega^\pi = 1/2^\pm$. On the other hand, the terms C_t^s are repulsive for the blocked levels with all values of Ω. The remaining time-odd terms are attractive for the blocked levels with high Ω and negligible for the blocked levels with low Ω.

We had the difficulty of convergence in the SkI3-HFB calculation when the $C_t^{\Delta s}$ terms are included. The difficulty also arises from the SLy4-HFB calculation when the C_t^s terms are omitted. These difficulties are mainly due to the strong $C_t^{\Delta s}$ terms and partly due to the large basis space of the calculation ($N_0 = 18$). For large $C_t^{\Delta s}$, the energy splitting between the time-reversed partners becomes large and a few of the quasi-particle states have negative energy.

Acknowledgments

We would like to thank K. Arita for many illuminating discussions. Numerical computation in this work was partly carried out at the Yukawa-Institute Computer Facility, Kyoto University.

References

[1] P. Aufmuth, K. Heilig and A. Steudel, At. Data Nucl. Data Tables 37 (1987) 455.

[2] P. Dabkiewicz, F. Buchinger, H. Fischer, H.-J.Kluge, H. Kremmling, T. Kühl, A. C. Müller and H. A. Schuessler, Phys. Lett. 82B (1979) 199.

[3] S. Frauendorf and V. V. Pashkevich, Phys. Lett. 55B (1975) 365.

[4] M. Calilliau, J. Letessier, H. Flocard and P. Quentin, Phys. Lett. 46B (1973) 11.

[5] S. Yoshida and N. Takigawa, Phys. Rev. C55 (1997) 1255.

[6] P. -G. Reinhard, C. Reiss, M. Bender, T. Bürvench, T. Cornelius and J. A. Maruhn, Hyp. Int. 127 (2000) 13.

[7] T. Nikšić, D. Vretenar, P. Ring and G. A. Lalazissis, Phys. Rev C65(2002) 054320.

[8] M. Beiner, H. Flocard, Nguyen Van Giai and P. Quentin, Nucl. Phys. A238 (1975) 29.

[9] P.-G. Reinhard and H. Flocard, Nucl. Phys. A584 (1995) 467.

[10] E. Chabanat, P. Bonche, P. Haensel, J. Meyer and R. Schaeffer, Nucl. Phys. A635 (1998) 231.

[11] H. J. Lipkin, Ann. Phys. (N.Y.) 9 (1960) 272.

[12] Y. Nogami, Phys. Rev. 134 (1964) B313.

[13] M. Bender, K. Rutz, P. -G. Reinhard and J. A. Maruhn, Eur. Phys. J. A8 (2000) 59.

[14] W. Satuła, R. Wyss and P. Magierski, Nucl. Phys. A578 (1994) 45.

[15] P. Ring and P. Schuck, *The Nuclear Many-Body Problem*, (Springer, Berlin, 1980).

[16] D. Vautherin and D. M. Brink, Phys. Rev. C5 (1972) 626.

[17] Y. M. Engel, D. M. Brink, K. Goeke, S. J. Krieger and D. Vautherin, Nucl. Phys. A249 (1975) 215.

[18] D. Vautherin, Phys. Rev. C7 (1973) 296.

[19] J. Dobaczewski, H. Flocard and J. Treiner, Nucl. Phys. A422 (1984) 103.

[20] M. V. Stoitsov, J. Dobaczewski, P. Ring and S. Pittel, Phys. Rev. C61 (2000) 034311.

[21] J. Dobaczewski, W. Nazarewicz and M. V. Stoitsov, Proc. on *The Nuclear Many-Body Problem 2001*, Brijuni National Park, Pula, Croatia, June 2-5, 2001 (nucl-th/0109073).

[22] K. Sugawara, Prog. Theor. Phys. 35 (1966) 44.

[23] P. Ring, R. Beck and H. J. Mang, Z. Phys. 231 (1970) 10.

[24] T. Duguet, P. Bonche, P. -H. Heenen and J. Meyer, Phys. Rev. C65 (2001) 014310, 014311.

[25] J. Dobaczewski and J. Dudek, Phys. Rev. C52 (1995) 1827, Phys Rev C55 (1997) E 3177.

[26] Nguyen Van Giai and H. Sagawa, Phys. Lett. 106B (1981) 379.

[27] J. Bartel, P. Quentin, M. Brack, C. Guet and H. -B. Håkansson, Nucl. Phys. A386 (1982) 79.

[28] B. Alex Brown, Phys. Rev. C58 (1998) 220.

[29] G. Audi and A. H. Wapstra, Nucl. Phys. A595 (1995) 409.

[30] A. Faessler, U. Götz, B. Slavov and T. Ledergerber, Phys. Lett. 39B (1972) 579.

[31] R. Bengtsson, T. Bengtsson, J. Dudek, G. Leander, W. Nazarewicz and J. Zhang, Phys. Lett. B183 (1987) 1.

Table 1: The time-odd coupling constants C_t^s and $C_t^{\Delta s}$ for the Skyrme SIII, SkI3 and SLy4 forces. The coupling constants C_t^s are given in MeV·fm^3, while $C_t^{\Delta s}$ are given in MeV·fm^5.

Force	$C_0^s(\rho=0)$	$C_0^s(\rho=\rho_{\rm NM})$	$C_1^s(\rho=0)$	$C_1^s(\rho=\rho_{\rm NM})$	$C_0^{\Delta s}$	$C_1^{\Delta s}$
SIII	14.109	56.401	141.094	98.802	17.031	17.031
SkI3	84.486	253.799	220.360	113.551	92.235	22.777
SLy4	–207.824	153.382	311.114	99.635	47.057	14.282

Table 2: Summary of the SIII-HFB calculation in keV. Notations; $\Omega^{\pi}_{\rm obl}$ and $\Omega^{\pi}_{\rm prol}$ denote the blocked level in the oblate and prolate minimum, respectively. $\Delta E^{\rm HFBE} = E^{\rm HFBE}_{\rm obl} - E^{\rm HFBE}_{\rm prol}$, $\Delta E^{\rm block} = E^{\rm block}_{\rm obl} - E^{\rm block}_{\rm prol}$, $\Delta E^{\rm pol} = E^{\rm pol}_{\rm obl} - E^{\rm pol}_{\rm prol}$, and $\Delta E^{\rm HFB} = E^{\rm HFB}_{\rm obl} - E^{\rm HFB}_{\rm prol}$. Polarization contributions are further divided into (i) the calculation with full time-odd terms, (ii) the calculation without C^s_t terms, (iii) the calculation without $C^{\Delta s}_t$ terms, and (iv) the calculation without both C^s_t and $C^{\Delta s}_t$ terms.

	N	100	101	102	103	104	105	106	107	108	109
	$\Delta E^{\rm HFBE}$	– 167	–110	– 68	– 76	– 152	–264	–470	–807	–1323	–962
	$\Omega^{\pi}_{\rm obl}$	–	$1/2^-$	–	$1/2^-$	–	$1/2^-$	–	$1/2^-$	–	$5/2^-$
	$\Omega^{\pi}_{\rm prol}$	–	$7/2^-$	–	$7/2^-$	–	$5/2^-$	–	$9/2^+$	–	$9/2^-$
	$E^{\rm block}_{\rm obl}$	–	1220	–	1263	–	1227	–	1317	–	1186
	$E^{\rm block}_{\rm prol}$	–	934	–	747	–	854	–	904	–	1412
	$\Delta E^{\rm block}$	–	286	–	516	–	373	–	413	–	–226
(i)	$E^{\rm pol}_{\rm obl}$	–	– 34	–	– 39	–	– 10	–	– 10	–	7
	$E^{\rm pol}_{\rm prol}$	–	32	–	31	–	36	–	47	–	36
	$\Delta E^{\rm pol}$	–	– 65	–	– 70	–	– 46	–	– 58	–	– 30
	$\Delta E^{\rm HFB}$	– 167	110	– 68	370	– 152	63	–470	–452	–1323	–1217
(ii)	$E^{\rm pol}_{\rm obl}$	–	–317	–	–328	–	–246	–	–250	–	–173
	$E^{\rm pol}_{\rm prol}$	–	–141	–	–102	–	–142	–	–111	–	–147
	$\Delta E^{\rm pol}$	–	–176	–	–226	–	–104	–	–139	–	– 26
	$\Delta E^{\rm HFB}$	–167	– 1	– 68	214	–152	5	–470	–533	–1323	–1214
(iii)	$E^{\rm pol}_{\rm obl}$	–	32	–	58	–	79	–	76	–	49
	$E^{\rm pol}_{\rm prol}$	–	60	–	58	–	73	–	73	–	61
	$\Delta E^{\rm pol}$	–	– 28	–	0	–	6	–	3	–	– 11
	$\Delta E^{\rm HFB}$	– 167	147	– 68	440	– 152	115	– 470	–391	–1323	–1199
(iv)	$E^{\rm pol}_{\rm obl}$	–	– 31	–	– 32	–	– 20	–	– 16	–	– 43
	$E^{\rm pol}_{\rm prol}$	–	– 66	–	– 64	–	– 41	–	– 41	–	– 80
	$\Delta E^{\rm pol}$	–	35	–	32	–	22	–	25	–	36
	$\Delta E^{\rm HFB}$	– 167	210	– 68	472	– 152	131	– 470	–370	–1323	–1152

Table 3: Summary of the SkI3-HFB calculation in keV. Notations are the same as those in Table 2.

	N	100	101	102	103	104	105	106	107	108	109
	$\Delta E^{\rm HFBE}$	– 54	20	– 93	– 90	– 76	– 106	–268	–628	–1159	–1855
	$\Omega^{\pi}_{\rm obl}$	–	$1/2^-$	–	$1/2^-$	–	$1/2^-$	–	$5/2^-$	–	$3/2^-$
	$\Omega^{\pi}_{\rm prol}$	–	$7/2^-$	–	$7/2^-$	–	$5/2^-$	–	$9/2^+$	–	$3/2^-$
	$E^{\rm block}_{\rm obl}$	–	1017	–	1124	–	1362	–	1098	–	1072
	$E^{\rm block}_{\rm prol}$	–	865	–	691	–	828	–	887	–	885
	$\Delta E^{\rm block}$	–	152	–	433	–	534	–	211	–	187
(iii)	$E^{\rm pol}_{\rm obl}$	–	124	–	122	–	116	–	73	–	87
	$E^{\rm pol}_{\rm prol}$	–	41	–	35	–	105	–	53	–	91
	$\Delta E^{\rm pol}$	–	84	–	87	–	11	–	20	–	– 4
	$\Delta E^{\rm HFB}$	– 54	256	– 93	430	– 76	440	–268	–397	–1159	–1673
(iv)	$E^{\rm pol}_{\rm obl}$	–	– 27	–	– 26	–	– 29	–	– 73	–	– 59
	$E^{\rm pol}_{\rm prol}$	–	–194	–	–193	–	–102	–	–147	–	–126
	$\Delta E^{\rm pol}$	–	168	–	167	–	73	–	74	–	67
	$\Delta E^{\rm HFB}$	– 54	340	– 93	509	– 76	501	–268	–343	–1159	–1602

Table 4: Summary of the SLy4-HFB calculation in keV. Notations are the same as those in Table 2.

	N	100	101	102	103	104	105	106	107	108	109
	$\Delta E^{\rm HFBE}$	– 181	– 219	– 276	– 428	– 670	– 968	–1337	–1457	–1530	–1601
	$\Omega^{\pi}_{\rm obl}$	–	$1/2^-$	–	$1/2^-$	–	$1/2^-$	–	$3/2^-$	–	$3/2^-$
	$\Omega^{\pi}_{\rm prol}$	–	$5/2^-$	–	$5/2^-$	–	$5/2^-$	–	$1/2^-$	–	$1/2^-$
	$E^{\rm block}_{\rm obl}$	–	1127	–	1109	–	1271	–	1169	–	1080
	$E^{\rm block}_{\rm prol}$	–	849	–	896	–	810	–	1276	–	1127
	$\Delta E^{\rm block}$	–	277	–	212	–	461	–	–107	–	– 47
(i)	$E^{\rm pol}_{\rm obl}$	–	– 82	–	– 68	–	– 69	–	– 16	–	– 14
	$E^{\rm pol}_{\rm prol}$	–	19	–	– 17	–	13	–	– 30	–	– 40
	$\Delta E^{\rm pol}$	–	–101	–	– 50	–	– 81	–	15	–	26
	$\Delta E^{\rm HFB}$	– 181	– 42	– 276	– 266	– 670	– 588	–1337	–1550	–1530	–1622
(iii)	$E^{\rm pol}_{\rm obl}$	–	127	–	117	–	131	–	91	–	85
	$E^{\rm pol}_{\rm prol}$	–	121	–	44	–	49	–	140	–	139
	$\Delta E^{\rm pol}$	–	7	–	74	–	82	–	– 49	–	– 55
	$\Delta E^{\rm HFB}$	– 181	65	– 276	– 142	– 670	– 425	–1337	–1631	–1530	–1702
(iv)	$E^{\rm pol}_{\rm obl}$	–	– 14	–	– 22	–	– 22	–	– 39	–	– 36
	$E^{\rm pol}_{\rm prol}$	–	– 66	–	– 101	–	–116	–	– 13	–	– 13
	$\Delta E^{\rm pol}$	–	52	–	79	–	94	–	– 25	–	– 22
	$\Delta E^{\rm HFB}$	– 181	110	– 276	– 137	– 670	– 413	–1337	–1589	–1530	–1670

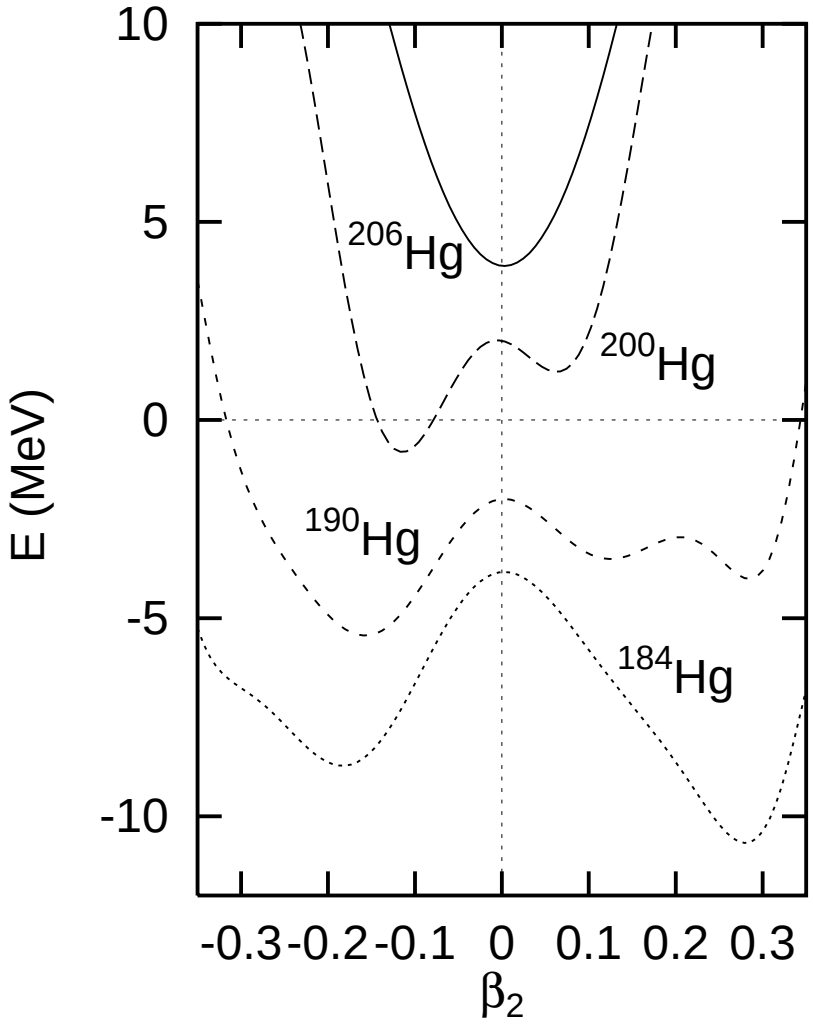

Figure 1: Deformation energy of Hg isotopes calculated by using the constraint SIII-HF method.

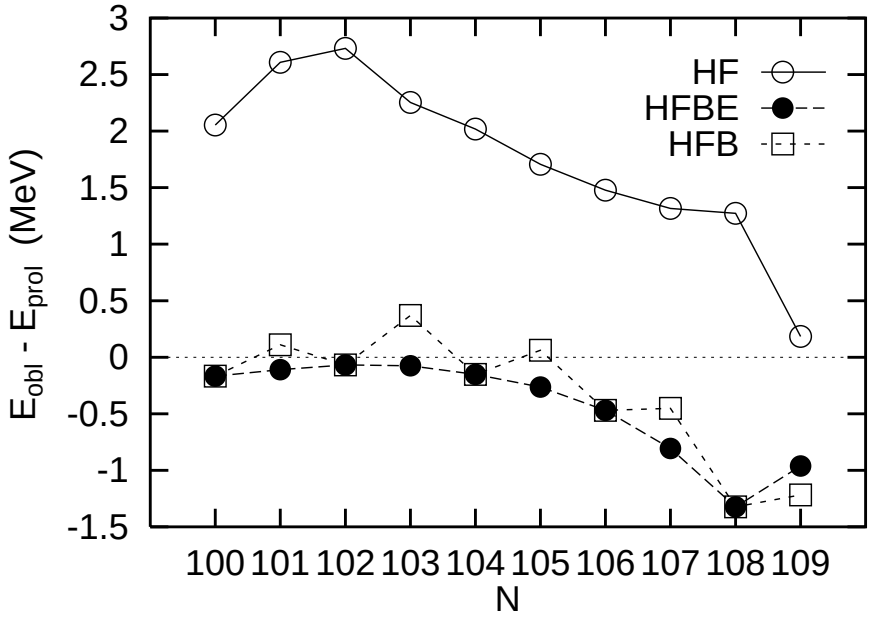

Figure 2: The oblate-prolate energy difference as a function of the neutron number N of Hg isotopes.

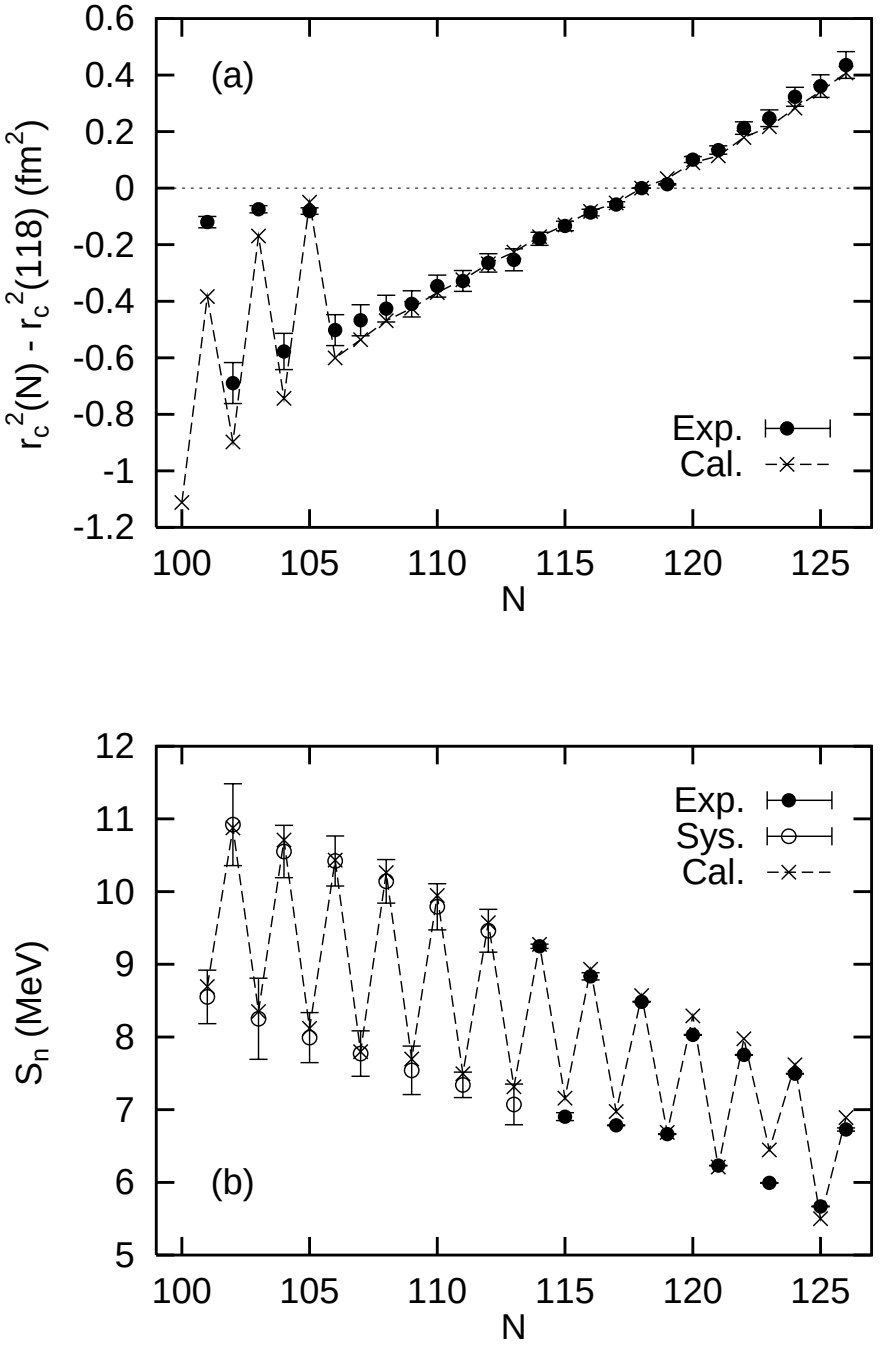

Figure 3: (a) The mean-square charge radius of $^{180-206}$Hg with respect to ^{198}Hg. (b) The one-neutron separation energy as a function of the neutron number N of Hg isotopes. Experiments are taken from [1] and [29], respectively. White circles in (b) denote the separation energy derived from systematic trends [29].

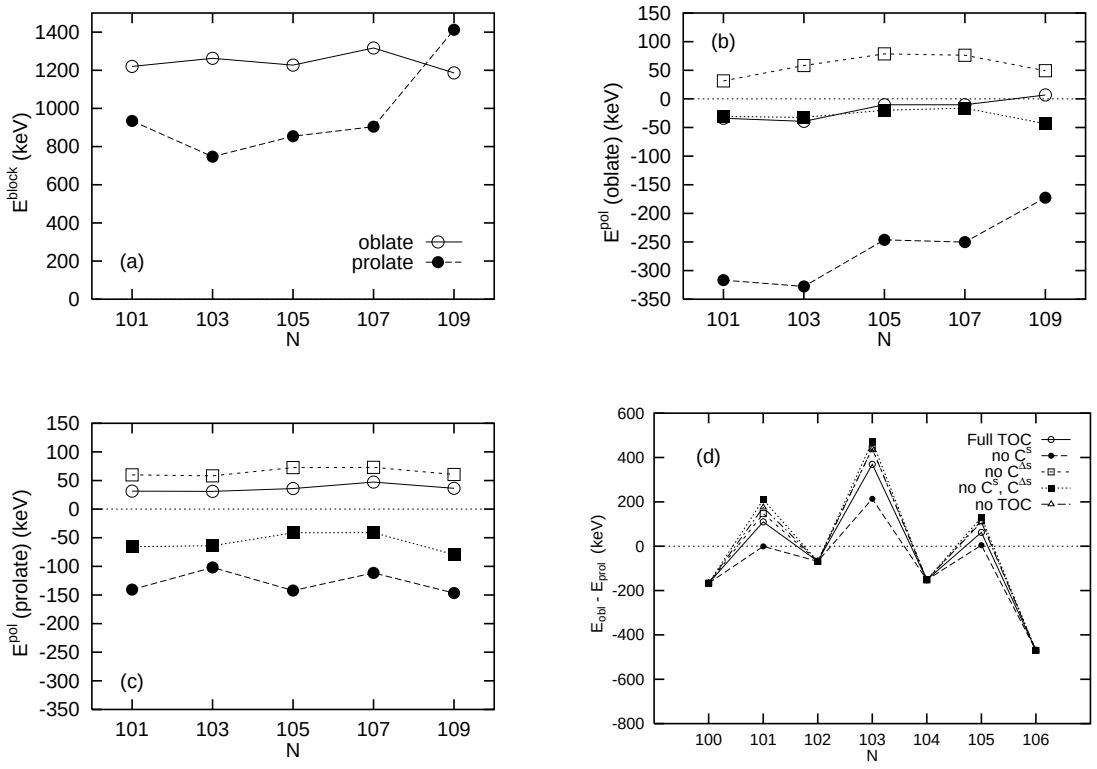

Figure 4: Results of the SIII-HFB calculation with the pairing parameters of $V_0 = -567$ MeV and $\rho_c = 0.145$ fm^{-3}. (a) The loss of pairing energy due to the self-consistent blocking of the Fermi level by the odd neutron. (b) The polarization energy in the oblate minimum. (c) The polarization energy in the prolate minimum. (d) The oblate-prolate energy difference. Case (i): the calculation with full time-odd terms (white circle). Case (ii): the calculation without the C_t^s terms (black circle). Case (iii): the calculation without the $C_t^{\Delta s}$ terms (white square). Case (iv): the calculation without both C_t^s and $C_t^{\Delta s}$ terms (black square). The calculation with no time-odd components is shown in white triangle.

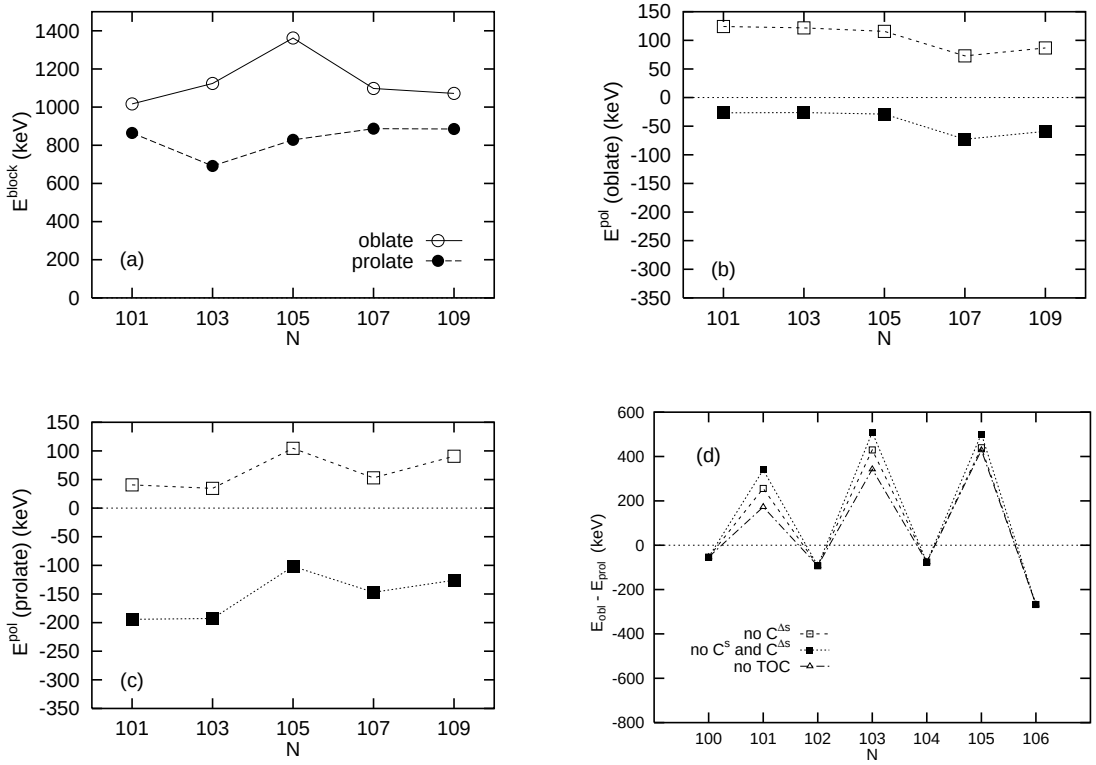

Figure 5: Results of the SkI3-HFB calculation with the pairing parameters of $V_0 = -560$ MeV and $\rho_c = 0.158$ fm^{-3}. (a) The loss of pairing energy due to the self-consistent blocking of the Fermi level by the odd neutron. (b) The polarization energy in the oblate minimum. (c) The polarization energy in the prolate minimum. (d) The oblate-prolate energy difference. Case (iii): the calculation without the $C_t^{\Delta s}$ terms (white square). Case (iv): the calculation without both C_t^s and $C_t^{\Delta s}$ terms (black square). The calculation with no time-odd components is also shown in white triangle.

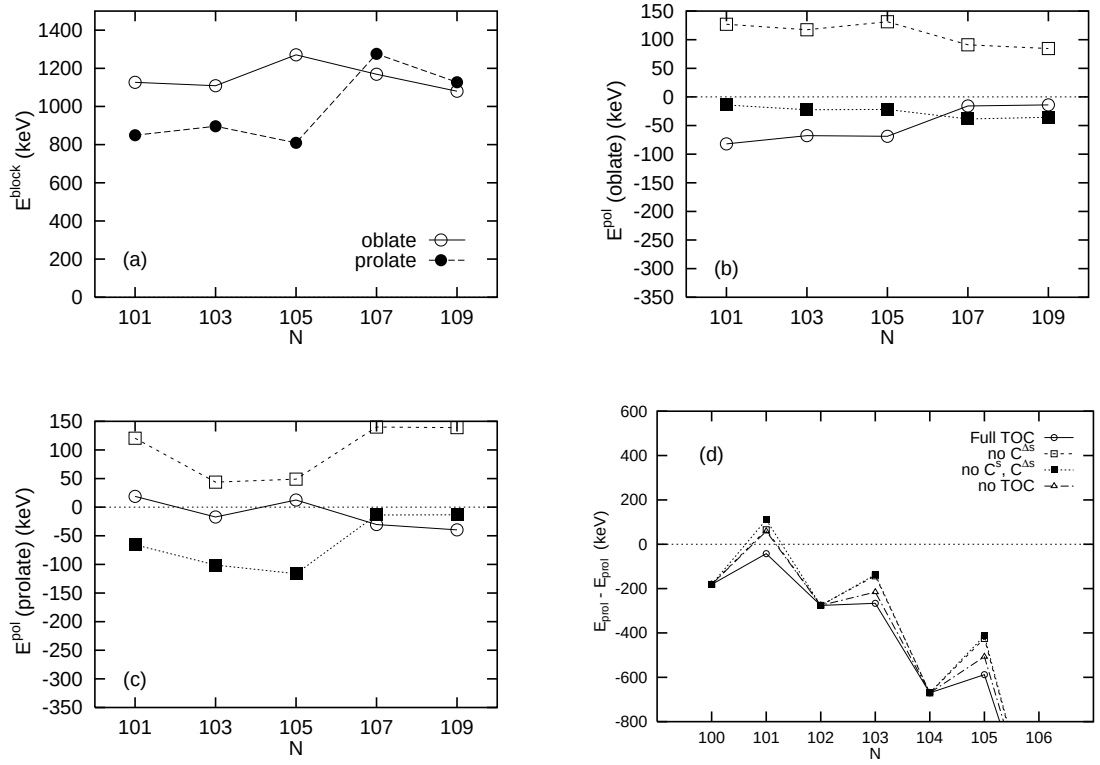

Figure 6: Results of the SLy4-HFB calculation with the pairing parameters of $V_0 = -500$ MeV and $\rho_c = 0.160$ fm^{-3}. (a) The loss of pairing energy due to the self-consistent blocking of the Fermi level by the odd neutron. (b) The polarization energy in the oblate minimum. (c) The polarization energy in the prolate minimum. (d) The oblate-prolate energy difference. Case (i): the calculation with full time-odd terms (white circle). Case (iii): the calculation without the $C_t^{\Delta s}$ terms (white square). Case (iv): the calculation without both C_t^s and $C_t^{\Delta s}$ terms (black square). The calculation with no time-odd components is also shown in white triangle.

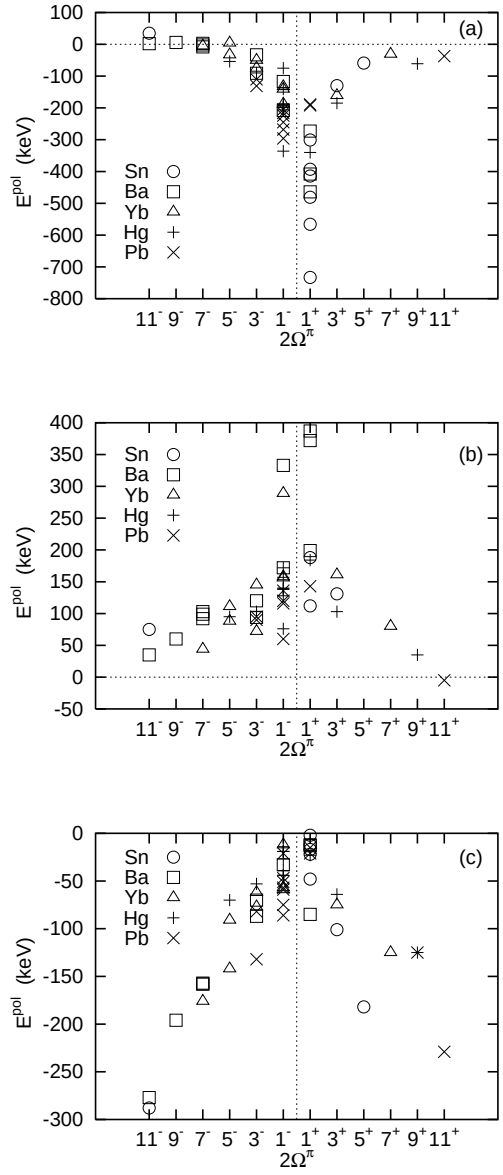

Figure 7: The time-odd mean-field energy calculated by the SkI3-HFB method with the basis space of $N_0 = 10$. The energy is plotted against $2\Omega^{\pm}$, twice of the component of neutron angular momentum along the symmetry axis. (a) The calculation with full time-odd terms, (b) the calculation without the $C_t^{\Delta s}$ terms, and (c) the calculation without both $C_t^{\Delta s}$ and C_t^s terms.